Linking crystallographic model and data quality

P. Andrew Karplus[1] and **Kay Diederichs**[*,2]

[1]Department of Biochemistry & Biophysics, Oregon State University, Corvallis, OR 97331, USA

[2]University of Konstanz, Faculty of Biology, Box 647, D-78457 Konstanz, Germany

Abstract

In macromolecular X-ray crystallography, refinement R values measure the agreement between observed and calculated data. Analogously, R_{merge} values reporting on the agreement between multiple measurements of a given reflection are used to assess data quality. We here show that despite their widespread use, R_{merge} values are poorly suited for determining the high resolution limit, and that current standard protocols discard much useful data. We introduce a statistic that estimates the correlation of an observed dataset with the underlying (not measurable) true signal; this quantity, CC*, provides a single statistically-valid guide for deciding which data are useful. CC* also can be used to assess model and data quality on the same scale and this reveals when data quality is limiting model improvement.

Accurately determined protein structures provide insight into how biology functions at the molecular level and also guide the development of new drugs and protein-based nanomachines and technologies. The large majority of protein structures are determined by X-ray crystallography, where measured diffraction data is used to derive a molecular model. Surprisingly, despite decades of methodology development, the question of how to select the resolution cutoff of a crystallographic dataset is still controversial and the link between the quality of the data and the quality of the derived molecular model is poorly understood. Here, we describe a statistical guide that allows assessment of the resolution limit that will optimize model quality.

The measured data in X-ray crystallography are the intensities of reflections, and these yield structure factor amplitudes each with unique h, k, l indices which define the lattice planes. The standard indicator for assessing the agreement of a refined model with the data is the crystallographic R value, defined as

$$R = \frac{\sum_{hkl} |F_{obs}(hkl) - F_{calc}(hkl)|}{\sum_{hkl} F_{obs}(hkl)} \tag{1}$$

with $F_{obs}(hkl)$ and $F_{calc}(hkl)$ being the observed and calculated structure factor amplitudes, respectively. R is 0.0 for perfect agreement with the data, and R is near 0.59 for a random model (1). Because R can be made arbitrarily low for models having sufficient parameters

to overfit the data, Brünger (2) introduced R_{free} as a cross-validated R based on a small subset of reflections not used during refinement. The R for the larger "working" set of reflections is then referred to as R_{work}.

Crystallographic data quality is commonly assessed by an analogous indicator R_{merge} (originally [3] R_{sym}), which measures the spread of n independent measurements of the intensity of a reflection, $I_i(hkl)$, around their average, $\bar{I}(hkl)$:

$$R_{merge} = \frac{\sum\limits_{hkl} \sum\limits_{i=1}^{n} |I_i(hkl) - \bar{I}(hkl)|}{\sum\limits_{hkl} \sum\limits_{i=1}^{n} I_i(hkl)} \qquad (2)$$

In 1997, it was discovered that because $I_i(hkl)$ influence $\bar{I}(hkl)$, the R_{merge} definition must be adjusted by a factor of $\sqrt{\frac{n}{n-1}}$ to give values that are independent of the multiplicity (4). The multiplicity-corrected version, called R_{meas}, reliably reports on the consistency of the individual measurements. A further variant, R_{pim} (5), reports on the expected precision of $\bar{I}(hkl)$ and is lower by a factor of $\frac{1}{\sqrt{n}}$ factor compared to R_{meas}. Because the strength of diffraction decreases with resolution, a high-resolution cutoff is applied to discard data considered so weak that their inclusion might degrade the quality of the resulting model. Data are typically truncated at a resolution before the R_{merge} (or R_{meas}) value exceeds ~0.6 - 0.8 and before the empirical signal-to-noise ratio, $< \bar{I}/\sigma(\bar{I}) >$, drops below ~2.0 (6) (Figure S1). The uncertainty associated with these criteria is illustrated by a recent review that concluded "an appropriate choice of resolution cutoff is difficult and sometimes seems to be performed mainly to satisfy referees" (6).

That these criteria result in high resolution cutoffs that are too conservative is illustrated here using an example dataset (**EXP**) collected for a cysteine-bound complex of cysteine dioxygenase (CDO); the **EXP** data has about 15-fold weaker intensity than the data originally used to determine the structure at 1.42 Å resolution (PDB 3ELN; $R_{work}/R_{free}=0.135/0.177$) (7, 8). Standardized model refinements starting with a 1.5 Å resolution unliganded CDO structure (PDB code 2B5H (9)) were carried out against the **EXP** data for a series of high resolution cutoffs between 2.0 and 1.42 Å resolution (Table S1). As R value comparisons are only meaningful if calculated at the same resolution, paired refinements done with adjacent resolution limits were evaluated using R_{work} and R_{free} values calculated at the poorer resolution limit. Improvement is indicated by drops in R_{free} or increases in R_{work} at the same R_{free} (meaning the model is less overfit). This analysis revealed that every step of added data improved the resulting model (Figure 1). Consistent with this, difference Fourier maps show a similar trend in signal versus resolution (Figure S2), and geometric parameters of the resulting models improve with resolution (Table S2).

The proven value of the data out to 1.42 Å resolution contrasts strongly with the R_{meas} and $< \bar{I}/\sigma(\bar{I}) >$ values at that resolution (> 4.0 and ~ 0.3, respectively; Figure 2), which are far beyond the limits currently associated with useful data. Applying the typical standards described above, this dataset would have been truncated at ~1.8 Å resolution, halving the number of unique reflections in the dataset (Table S1) and yielding a worse model.

It is striking to observe the different behavior at high resolution of the crystallographic versus the data-quality R values, with the one remaining below 0.40 and the other diverging toward infinity (Figure 2). Consideration of the R_{merge} formula rationalizes this divergence, as the denominator (the average net intensity) approaches zero at high resolution while the numerator becomes dominated by background noise and is essentially constant. Thus, despite their similar names and mathematical definitions, data-quality R values *are not* comparable to R values from model refinement, and there is no valid basis for the commonly applied criterion that data are not useful beyond a resolution where R_{meas} (or

R_{merge} or R_{pim}) rises above ~0.6. As suggested by Wang (10), $<\bar{I}/\sigma\left(\bar{I}\right)>$ at a much lower level than generally recommended could be used to define the cutoff, but this has the

problem that $\sigma\left(\bar{I}\right)$ values can be misestimated (6, 11).

With current standards not serving as reliable guides for selecting a high resolution cutoff, we investigated the use of the Pearson correlation coefficient (CC) (12) as a parameter that could potentially assess both data accuracy and the agreement of model and data on a common scale. Pearson's CC is already used in crystallography, in that a CC value of 0.3 between independent measurements of anomalous signals has become the recommended criterion for selecting the high-resolution cutoff of the data to be used for defining the locations of the anomalous scatterers (13). Following a procedure suggested earlier (4), we divided the unmerged *EXP* data into two parts, each containing a random half of the measurements of each unique reflection. Then, the CC was calculated between the average intensities of each subset. This quantity, denoted $CC_{1/2}$, is near 1.0 at low resolution and drops to near 0.1 at high resolution (Figure 3). According to the Student's t-test (12), the $CC_{1/2}$ of 0.09 for the ~2100 reflection pairs in the highest resolution bin is significantly different from zero (P = $2*10^{-5}$).

This high significance occurs even though $CC_{1/2}$ should be expected to underestimate the information content of the data. This is because for weak data, $CC_{1/2}$ measures the correlation of one noisy dataset (the first half-dataset) with another noisy dataset (the other half-dataset), whereas the true level of signal would be measured by what could be called CC_{true}, the correlation of the averaged dataset (less noisy due to the extra averaging) with the noise-free true signal. Although the true signal would normally not be known, for the *EXP* test case, the 3ELN data provides a reference that has much lower noise and should be much closer to the underlying true data. The CC calculated between the *EXP* and 3ELN datasets is indeed uniformly higher than $CC_{1/2}$ (Figure 3), dropping only to 0.31 in the highest resolution bin (Student's t-test P = 10^{-64}).

We next sought an analytical relationship between $CC_{1/2}$ and CC_{true}. Using only the assumption that errors in the two half-datasets are random and, on average, of similar size (see Supplementary Text), we derived the relationship

$$CC^{*}= \sqrt{\frac{2CC_{1/2}}{1+CC_{1/2}}} \tag{3}$$

where CC* estimates the value of CC_{true}, based on a finite size sample. Eqn 3 has been used in electron microscopy studies for a similar purpose (14), and is also related to the Spearman-Brown prophecy formula used in psychometrics to predict what test length is required to achieve a certain level of reliability (15). CC*, when computed with eqn 3, agrees reasonably well with the CC for the *EXP* data compared with the 3ELN reference data, showing that systematic factors influencing a real dataset are not large enough to greatly perturb this relationship (Figure 4A). CC* provides a statistic that not only assesses

data quality, but also allows direct comparison of crystallographic model quality and data quality on the same scale. In particular, CC_{work} and CC_{free} – the standard and cross-validated correlations of the experimental intensities with the intensities calculated from the refined molecular model – can be directly compared with CC* (Figure 4B). A CC_{work} larger than CC* implies overfitting, since in that case the model agrees better with the experimental data than the true signal does. A CC_{free} smaller than CC* (such as is seen at low resolution) indicates that the model does not account for all of the signal in the data. A CC_{free} closely matching CC*, such as at high resolution in Figure 4B, implies that data quality is limiting model improvement. In this region the model, which was refined against *EXP*, correlates much better with the more accurate 3ELN than with the *EXP* data (Figure 4B), showing that as is common for parsimonious models (16), the constructed molecular model is a better predictor of the true signal than is the experimental data from which it was derived. On a related point, because current estimates of a model's coordinate error do not take the data errors into account (17-19), the model accuracy is actually better than these methods indicate.

We verified, using a simulated dataset (20), that these findings are not specific to the *EXP* data (Tables S3, S4 and S5, and Figure S3). Thus, CC* (or $CC_{1/2}$) is a robust, statistically informative quantity useful for defining the high-resolution cutoff in crystallography. These examples show that with current data reduction and refinement protocols, it is justified to include data out to well beyond currently employed cutoff criteria (Figure S4), because the data at these lower signal levels do not degrade the model, but actually improve it. Advances in data processing and refinement procedures, which until now have not been optimized for handling such weak data, may lead to further improvements in model accuracy. Finally, we emphasize that the analytical relation (eqn 3) between $CC_{1/2}$ and CC* is general and thus CC* may have similar applications for data and model quality assessment in other fields of science involving multiply measured data.

Supplementary Material

Refer to Web version on PubMed Central for supplementary material.

Acknowledgments

References and Notes

1. Wilson AJC. Largest likely values for the reliability index. Acta Cryst. 1950; 3:397–398.

2. Brünger ATB. Free R value: a novel statistical quantity for assessing the accuracy of crystal structures. Nature. 1992; 355:472. [PubMed: 18481394]

3. Arndt UW, Crowther RA, Mallett JFW. A computer-linked cathode-ray tube microdensitometer for X-ray crystallography. J. Phys. E: Sci. Instrum. 1968; 1:510.

4. Diederichs K, Karplus PA. Improved R-factors for diffraction data analysis in macromolecular crystallography. Nature Structural Biology. 1997; 4:269.

5. Weiss MS. Global indicators of X-ray data quality. J. Appl. Cryst. 2001; 34:130.

6. Evans PR. An introduction to data reduction: space-group determination, scaling and intensity statistics. Acta Cryst. 2011; D67:282.

7. Simmons CR, et al. A Putative Fe2+-Bound Persulfenate Intermediate in Cysteine Dioxygenase. Biochemistry. 2008; 47:11390. [PubMed: 18847220]

8. Materials and methods are available as supplementary material on Science Online.

9. Simmons CR, et al. Crystal Structure of Mammalian Cysteine Dioxygenase. J. Biol. Chem. 2006; 281:18723. [PubMed: 16611640]

10. Wang J. Inclusion of weak high-resolution X-ray data for improvement of a group II intron structure. Acta Cryst. 2010; D66:988.

11. Evans P. Scaling and assessment of data quality. Acta Cryst. 2006; D62:72.

12. Rahman, NA. A Course in Theoretical Statistics. Charles Griffin and Company; 1968.

13. Schneider TR, Sheldrick GM. Substructure solution with SHELXD. Acta Cryst. 2002; D58:1772.

14. Rosenthal PB, Henderson R. Optimal Determination of Particle Orientation, Absolute Hand, and Contrast Loss in Single-particle Electron Cryomicroscopy. J. Mol. Biol. 2003; 333:721. [PubMed: 14568533]

15. Bobko, P. Correlation and Regression: Applications for Industrial Organizational Psychology and Management. Sage Publications; Thousand Oaks, London, New Delhi: 2001.

16. Gauch HG Jr. Prediction, Parsimony and noise. American Scientist. 1993; 81:468.

17. Luzzatti V. Resolution d'une structure cristalline lorsque les positions d'une partie des atoms sont connues: Traitement statistique. Acta Cryst. 1953; 6:142.

18. Cruickshank DWJ. Remarks about protein structure precision. Acta Cryst. 1999; D55:583.

19. Steiner RA, Lebedev AA, Murshudov GN. Fisher's information in maximum-likelihood macromolecular crystallographic refinement. Acta Cryst. 2003; D59:2114.

20. Diederichs K. Simulation of X-ray frames from macromolecular crystals using a ray-tracing approach. Acta Cryst. 2009; D65:535.

21. Fisher, R. Statistical methods for research workers. Oliver and Boyd; Edinburgh: 1925. p. §33-34.

22. Ten independent random partitionings of the data into the two subsets for calculating $CC_{1/2}$ yielded standard deviations of <0.02 in all resolution ranges, and agreed reasonably with the expected standard error as calculated by $\sigma(CC) = (1 - CC^2)/ (n-1)$ where n is the number of observations contributing to the CC calculation (21).
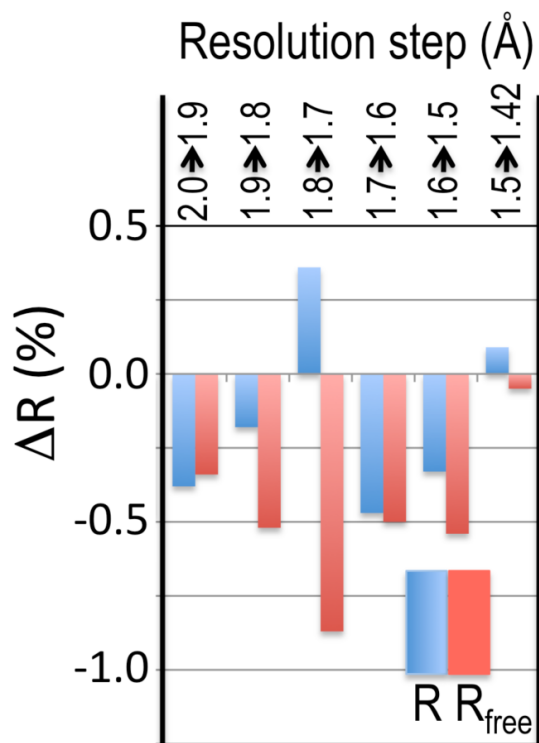
Figure 1.

Higher resolution data, even if weak, improves refinement behaviour. For each incremental step of resolution from X->Y (top legend), the pair of bars gives the changes in overall R_{work} (blue) and R_{free} (red) for the model refined at resolution Y with respect to those for the model refined at resolution X, with both R values calculated at resolution X. The first pair of bars shows that R_{work} and R_{free} dropped 0.38 and 0.34% upon isotropic refinement, respectively, when the refinement resolution limit was extended from 2.0 to 1.9 Å; the other pairs of bars show the improvement upon anisotropic refinement.
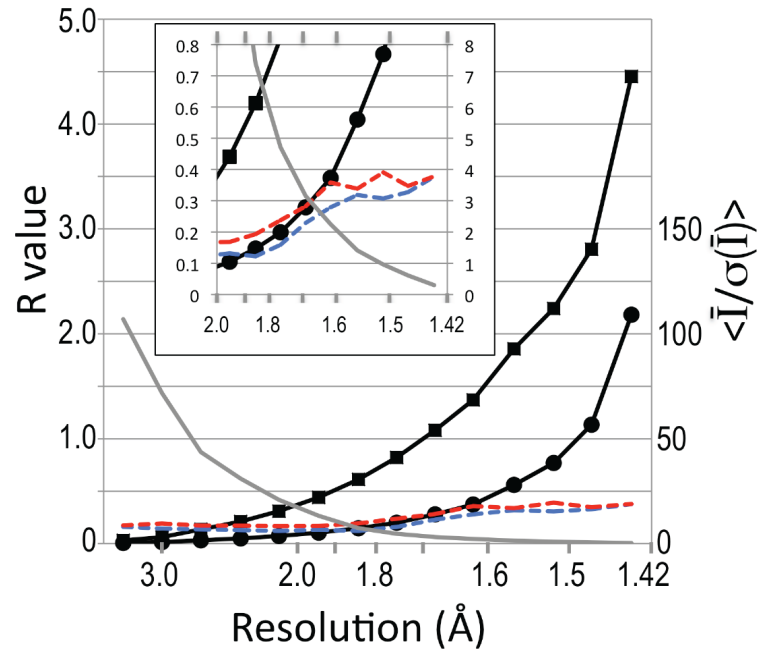
Figure 2.
Data quality R values behave differently than those from crystallographic refinement, and useful data extend well beyond what standard cutoff criteria would suggest. R_{meas} (squares) and R_{pim} (circles) are compared with R_{work} (blue) and R_{free} (red) from 1.42 Å resolution

refinements against the ***EXP*** dataset. $< \bar{I} / \sigma(\bar{I}) >$ (grey X) is also plotted. Inset is a close-up of the plot beyond 2 Å resolution.
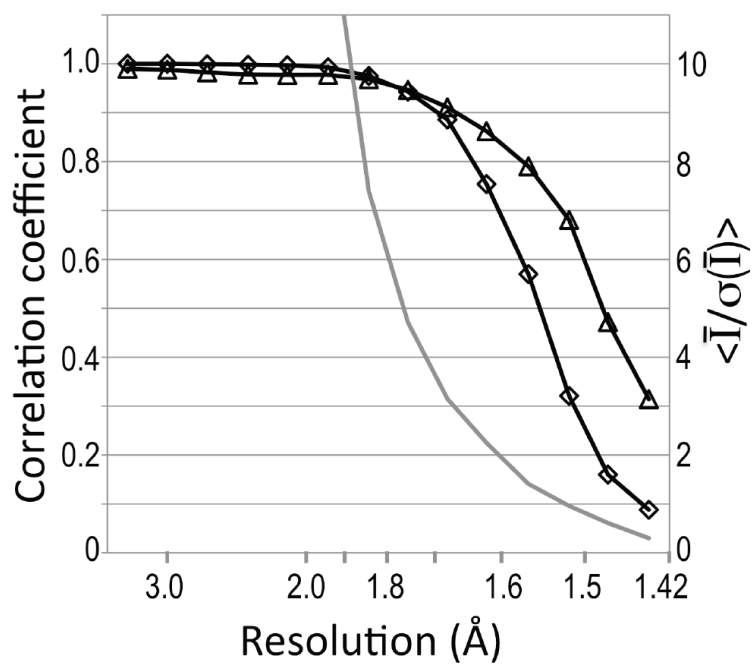
Figure 3.
Signal as a function of resolution as measured by correlation coefficients. Plotted as a function of resolution for the ***EXP*** data is $CC_{1/2}$ (diamonds) and the CC for a comparison with the 3ELN reference dataset (triangles). $< \bar{I} /\sigma\left(\bar{I}\right)>$ (grey) is also shown. All determined $CC_{1/2}$ values shown have expected standard errors of <0.025 (21, 22).
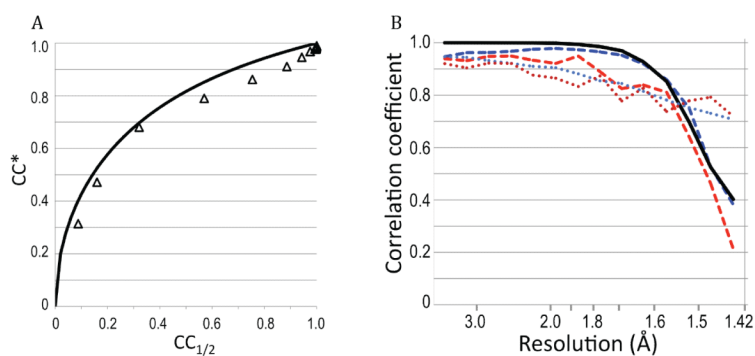
Figure 4.
The $CC_{1/2}$ / CC* relationship and the utility of comparing CC* with CC_{work} and CC_{free} from a refined model. (A) Plotted is the analytical relationship (eqn. 3) between $CC_{1/2}$ and CC* (black curve). Also roughly following the CC* curve are the CC values for the **EXP** data compared with 3ELN (triangles) as a function of $CC_{1/2}$. (B) Plotted as a function of resolution are CC* (black solid) for the **EXP** dataset as well as CC_{work} (blue dashed) and CC_{free} (red dashed) calculated on intensities from the 1.42 Å refined model. Also shown are CC_{work} (blue dotted) and CC_{free} (red dotted) between the 1.42 Å refined model and the 3ELN dataset.